Dalton Transactions

Homogeneous versus MOF-supported catalysis: A direct comparison of catalytic hydroboration at Ni tripodal P_3E (E = Si, Ge) complexes

Journal:	*Dalton Transactions*
Manuscript ID	DT-ART-05-2023-001328.R1
Article Type:	Paper
Date Submitted by the Author:	22-May-2023
Complete List of Authors:	Barrios-Vargas, Luz; Mississippi State University, Chemistry Abeynayake, Niroshani; Mississippi State University, Chemistry Secrist, Carlee; Mississippi State University, Chemistry Le, Nghia; Vietnam National University Ho Chi Minh City, chemistry; Webster, Charles Edwin; Mississippi State University, Chemistry Donnadieu, Bruno; Mississippi State University, Department of Chemistry Kaphan, David M; Argonne National Laboratory, Roy, Amitava; Louisiana State University, Center for Advanced Microstructures and Devices Ibarra, Ilich; Universidad Nacional Autónoma de México, Instituto de Investigaciones en Materiales Montiel-Palma, Virginia; Mississippi State University, Chemistry

ARTICLE

Homogeneous versus MOF-supported catalysis: A direct comparison of catalytic hydroboration at Ni tripodal P_3E (E = Si, Ge) complexes

Received 00th January 20xx,
Accepted 00th January 20xx

DOI: 10.1039/x0xx00000x

Luz J. Barrios-Vargas,[a,†] Niroshani S. Abeynayake,[a,†] Carlee Secrist,[a] Nghia Le,[a,†] Charles Edwin Webster,[a] Bruno Donnadieu,[a] David M. Kaphan,[b] Amitava D. Roy, [c] Ilich A. Ibarra[d] and Virginia Montiel-Palma*[a]

MOF material NU-1000 was employed to host Ni tripodal complexes prepared from new organometallic precursors [HNi(κ^4(*E,P,P,P*)-E(*o*-$C_6H_4CH_2PPh_2)_3$], E = Si (**Ni-1**), Ge (**Ni-2**). The new heterogenous catalytic materials, **Ni-1@NU-1000** and **Ni-2@NU-1000** show the advantages of both homogenous and heterogeneous catalysts. They catalyze the hydroboration of aldehydes and ketones more efficiently than the homogenous **Ni-1** and **Ni-2**, under aerobic conditions, and allowing recyclability of the catalyst.

Introduction

The laboratory design and synthesis of new efficient catalysts for the transformation of hydrocarbons into valuable products is a path to advance the understanding of catalytic cycles, ultimately leading to a more rational use of nonrenewable resources. Metal-organic frameworks, MOFs, consisting of inorganic nodes and organic linkers forming reticular materials with high surface areas,[1] afford fascinating entries to single-site heterogeneous catalysts, SSHCs. MOFs are advantageous over other traditional supports in that they provide a more extensive scope for structural variation and the opportunity of investigating different platforms, strategies[2-4] and kinetic pathways.[5] Elegant examples of MOF supported SSHCs demonstrate improvement of the catalytic performance in comparison to their homogeneous counterparts.[5-9] For example, mesoporous Zr-based NU-1000[10] allows the uniform installation of Ni ions revealing the higher activity and stability of the resulting material as catalyst for ethylene hydrogenation.[11] The enhanced catalytic virtues are attributed to the prevention of active site migration and sintering.[4, 8]

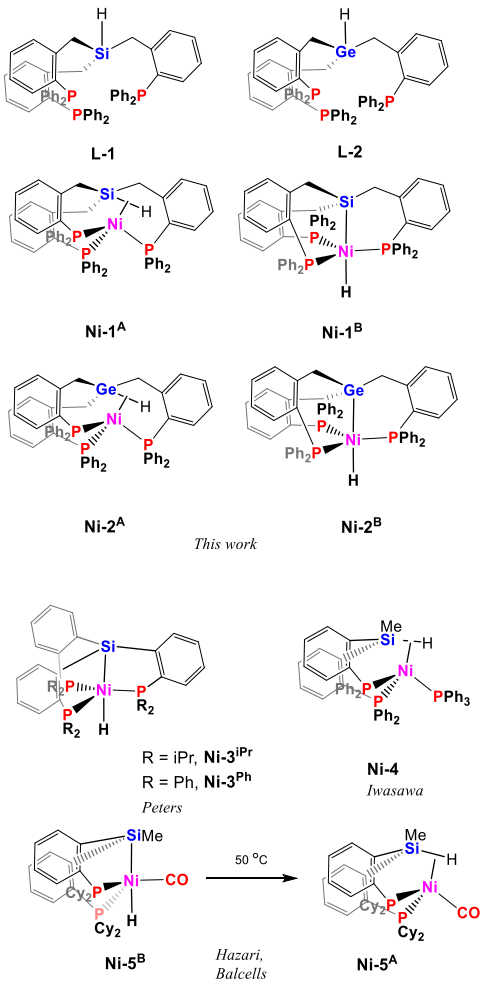

Chart 1. Structures of complexes synthesized and literature examples discussed in this work.

[a.] *Department of Chemistry, Mississippi State University, Mississippi State, Mississippi 39762, United States. E-mail: vmontiel@chemistry.msstate.edu*
[b.] *Chemical Sciences and Engineering Division, Argonne National Laboratory, Lemont, Illinois 60439, United States.*
[c.] *Center for Advanced Microstructures and Devices (CAMD), Louisiana State University, Baton Rouge, Louisiana 70806, United States*
[d.] *Laboratorio de Fisicoquímica y Reactividad de Superficies (LaFReS), Instituto de Investigaciones en Materiales, Universidad Nacional Autónoma de México, Circuito Exterior s/n, CU, Coyoacán, 04510, Ciudad de México, Mexico.*
† These authors contributed equally.

Electronic Supplementary Information (ESI) available: Full experimental and computational details. Single crystal X-ray diffraction details of complexes **Ni-1** and **Ni-2**, CCDC 2247469 and 2247468. See DOI: 10.1039/x0xx00000x

Although many SSHCs have been reported as derived from the deposition of organometallic complexes onto MOFs, there are only limited examples of transition metal complexes that bear "tailor-made" ligands which could allow a finer and/or systematic tuning of the steric and electronic properties of the grafted organometallic fragments.[9, 12, 13] Herein, we present a direct comparison of an organometallic Ni system that is active as homogeneous catalyst for aldehyde hydroboration and its corresponding MOF grafted heterogenous counterpart which shows enhanced catalytic properties, allows recyclability and permits catalysis to be performed under aerobic conditions.

Results and discussion

Synthesis of ligands [HSi(*o*-$C_6H_4CH_2P(C_6H_5)_2)_3$] (L1) and [HGe(*o*-$C_6H_4CH_2P(C_6H_5)_2)_3$] (L2).

Access to the tripodal triphosphino-E-hydride ligands of formula [HE(*o*-$C_6H_4CH_2PPh_2)_3$], E = Si[14] (**L1**) and Ge (**L2**) (**Chart 1**) was achieved from organolithiated diphenyl(*o*-tolyl)phosphine.[14, 15] **L1** had previously been reported by Stobart and coworkers.[14] In the new semirigid germylphosphine ligand **L2**, HGe(*o*-$C_6H_4CH_2PPh_2)_3$], the $\nu_{Ge\text{-}H}$ stretching vibration appears at 2065 cm^{-1}, midway between the Ge-H stretching vibration of 2037 cm^{-1} in Ph_3GeH,[16] and that of the rigid analogue [HGe(*o*-$C_6H_4PPh_2)_3$], reported by Braun and coworkers, which appears at 2092 cm^{-1}.[17] In **L2**, a multiplet for the Ge bound hydrogen appears at δ 4.85 in the ^{1}H NMR spectrum in C_6D_6, considerably shielded from that in the rigid compound at δ 7.19 and close to the chemical shift of the hydrogen bound to Si in **L1** at δ 4.22 In **L2**, the benzylic methylene appears at δ 2.92, slightly deshielded when compared with **L1** at δ 2.49.

Synthesis, characterization, and proposed structures of [HNi(κ^4(*E,P,P,P*)-E(*o*-$C_6H_4CH_2PPh_2)_3$] (E = Si, Ni-1; E= Ge, Ni-2): adoption of different structures in solid state and in solution.

Equimolar reaction of ligands **L1** or **L2** with $Ni(PPh_3)_4$ resulted after workup in the isolation of new complexes **Ni-1** and **Ni-2** in good yields. The complexes were fully characterized by spectroscopic methods and by single-crystal X-ray diffraction. The silicon complex **Ni-1**, is the semirigid analogue of [HNi(κ^4(*Si,P,P,P*)-Si(*o*-$C_6H_4PPh_2)_3$] previously proposed by Peters and coworkers (**Ni-3^{Ph}**, **Chart 1**) to exhibit a trigonal bipyramidal structure.[18, 19] The closely related tetrahedral [HNi(κ^3(*Si,P,P*)-SiMe(*o*-$C_6H_4PPh_2)_2$] (**Ni-4**, **Chart 1**) reported by Iwasawa and coworkers bears a pincer ligand and a non classical sigma silane ligand.[20, 21]

In the solid state, complexes **Ni-1** and **Ni-2** are isostructural by single crystal X-ray diffraction at 100 K (**Figure 1**). In each, the ligand coordinates to the metal through the three P and the E (Si, Ge) atoms, adopting a trigonal pyramidal geometry around Ni. The P atoms arrange in the equatorial plane with angles close to the ideal 120° and 90°. The apical position of the trigonal pyramid is occupied by either the Si or Ge atom. No significant variations in the Ni-P bond lengths are found by comparison with other related Ni complexes.[19, 22, 23] The Ni-Si distance in **Ni-1** of 2.246(2) Å is slightly longer than in **Ni-3^{iPr}** at 2.2014(5) Å[19] and shorter than in **Ni-4** at 2.2782(4) Å (**Chart 1**), falling within the typical region for other Ni^{II}-Si bonds (2.14-2.30 Å).[20, 24] In the **Ni-2** structure, the Ni-Ge bond distance of 2.2977(17) Å is comparable to other Ni germyl complexes and slightly longer than in **Ni-1**, as expected for its larger atomic radius.[25]

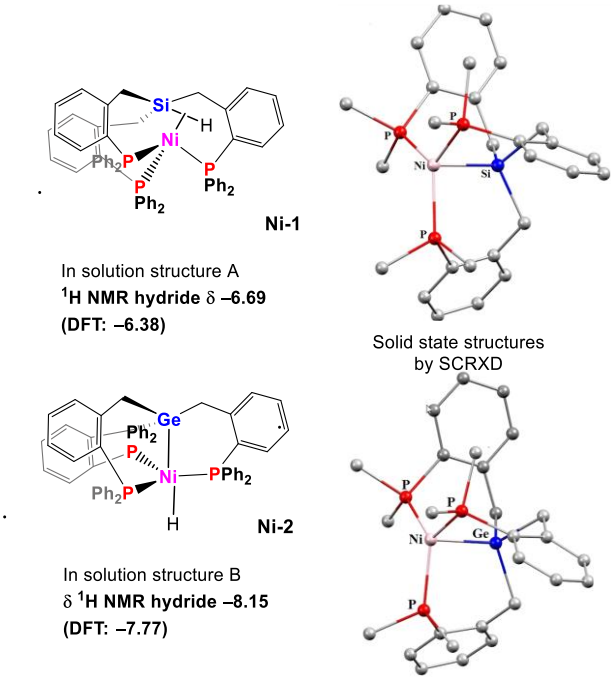

Figure 1. (**Left**) The proposed structures for **Ni-1** and **Ni-2** in solution with their corresponding hydride chemical shifts experimental and in brackets, computational. (**Right**) The solid-state structures by single crystal X-ray diffraction of **Ni-1** and **Ni-2**. Main bond distances (Å) and angles (°): for **Ni-1**, Ni1-Si1 2.246(2), Ni1-P1 2.1796(13), P1-Ni1-P1#2 119.985(2), P1-Ni1-Si1 90.74(4); for **Ni-2**, Ni1-Ge1 2.2977(17), Ni1-P1 2.1885(15), P1#2-Ni1-P1 119.9980(10), P1-Ni1-Ge1 90.25(5). In this work, we propose that the nature of the hydride is different in solution than in the solid state, with a higher contribution of the non classical sigma silane structure A in solution for **Ni-1** as shown by DFT computations.

Despite not being unambiguously located in the single crystal X ray diffraction structures of either complex **Ni-1** or **Ni-2**, the presence of a hydride bound to Ni was ascertained by NMR spectroscopy in solution. The ^{1}H NMR spectrum of the crystals of **Ni-1** in benzene-d_6 shows an upfield hydride signal at δ –6.69 as a quartet with $^2J_{HP}$ = 37 Hz and J_{HSi} = 52 Hz. Though the value of the Si-H coupling constant is indeed smaller than in other reported Ni^0(σ-SiH) complexes (77-105 Hz),[20, 26] it is still relatively large for a silyl hydride.[24] Hazari, Balcells, and coworkers observed the facile isomerization of **Ni-5^B** to **Ni-5^A** upon heating to only 50 °C[27] (**Charts 1** and **S1**).

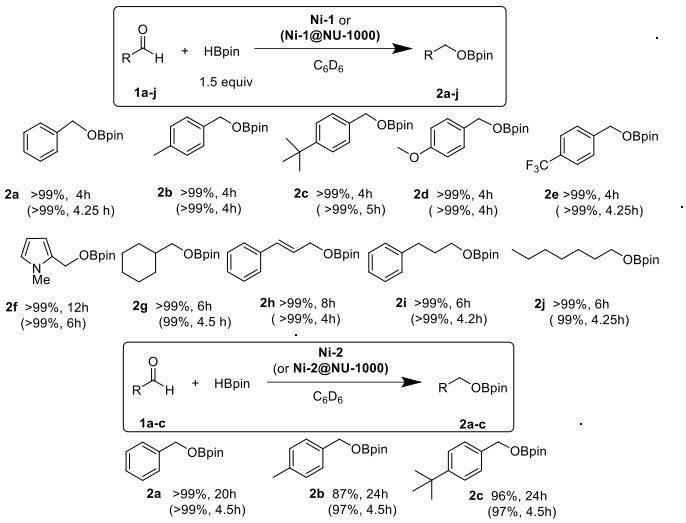

Chart 2. NMR yields and conversion times of the catalytic hydroboration of aldehydes by the four Ni catalysts. The hydroboration products are shown. Top shows the product yield and time of the catalysis by 2.0 mol% **Ni-1** at 50 °C and below, in brackets, the results using 0.30 mol% **Ni-1@NU-1000** at room temperature. The bottom shows the comparative NMR yields of the catalysis employing either 2 mol% **Ni-2** (50 °C) or 0.50 mol% **Ni-2@NU-1000** (RT, given in brackets).

Entry	Catalyst	Time / h	TON	TOF / h	Ref.
1	**Ni-1** [a]	4.0	50	12.5	*This work*
2	**Ni-1@NU-1000** [b]	4.2	333	79.3	*This work*
3	[Ni(iminophosphine)(allyl)]+ [b]	0.25	100	400	37
4	[Ni(bpy)(cod)] [b]	0.40	2833 [c]	7082	36
5	[Ni(POCN)H] [b]	0.08	20	250	38

Table 1. Comparison of the catalytic performance of Ni catalysts in this work and in literature references for the hydroboration of benzaldehyde. Data in C_6D_6. [a] 50 °C. [b] Room temperature. [c] After 0.40 h, only 85% NMR yield was reported. All catalysts achieve >99% conversion to the product at the indicated time except [Ni(bpy)(cod)] which achieves 85% conversion.

Entry	Catalyst	Time/ h	TON	TOF / h	Ref.
1	**Ni-1@NU-1000**[a]	8	317	40	*This work*
2	[Ni(iminophosphine)(allyl)]+ [b]	6	<2.5[d]	<0.42	37
3	[Ni(bpy)(cod)][c]	1	3100 [e]	3100	36
4	[Ni(POCN)H][c]	0.17	20	118	38

Table 2. Comparison of the catalytic performance of **Ni-1@NU-1000** and other Ni complexes reported in the literature for the hydroboration of methylphenylketone in C_6D_6. [a] 50 °C. [b] 60 °C. [c] Room temperature. [d] <5% product yield. [e] 93% product yield.

DFT calculations of Ni-1 and Ni-2.

Further insights into the nature of the hydride in both **Ni-1** and **Ni-2** in solution were obtained from DFT computations of the chemical shifts. In benzene, the classical hydride silyl (**Ni-1^B**) was computed at δ −8.18 ppm whereas the non classical sigma silane structure (**Ni-1^A**) gives δ −6.38, closer to the experimental value of δ −6.69 ppm (**Figures 1**, **S1** and **S2**). Further, in complex **Ni-2**, the hydride appears as a quartet at δ −8.15 in the ^{1}H NMR spectrum ($^2J_{HP}$ = 35 Hz), in close agreement with the DFT computed hydride germyl structure **Ni-2^B** at δ −7.77 ppm (**Figures 1**, **S1** and **S2**) and far from the computed non classical sigma germane **Ni-2^A** (δ −0.98 ppm). Considering the literature reports, the solution and solid state data and the DFT calculations, we propose that the geometry of **Ni-1** in benzene solution has a more important contribution of the elongated non classical sigma σ(Si-H) bond (structure A) whereas, structure B is more prevalent in **Ni-2** in solution.

Synthesis and characterization of grafted MOF materials Ni-1@NU-1000 and Ni-2@NU-1000.

Next, we post-synthetically grafted precursors **Ni-1** and **Ni-2** into in-house-synthesized NU-1000, first reported by Farha *et al* and consisting of pyrene linkers to Zr_6 clusters capped by four μ_3-hydroxo ligands.[28] The procedure for grafting involved soaking the MOF material into benzene solutions of the Ni complexes, as proposed by Lu and coworkers[29, 30] with some modifications.[31, 32] This method rendered new materials herein named **Ni-1@NU-1000** (**Figure S3**) and **Ni-2@NU-1000** (**Figure S5**). PXRD experiments performed on the materials demonstrated that the crystallinity of the unmodified NU-1000 was preserved upon metalation. Inductively coupled plasma-mass spectrometry, ICP-MS, determinations on acid digested samples of **Ni-1@NU-1000** revealed Ni metal loadings of 0.6 wt.% of Ni and 5.4 wt.% of Zr, corresponding to a Ni:Zr molar ratio of 0.96:6.0, thus, remarkably close to the ideal one Ni atom per Zr_6 cluster unit. Similarly, the grafting of **Ni-2** precursor and subsequent ICP-MS analysis of **Ni-2@NU-1000** gave a 1 wt.% of Ni, and 6.1 wt.% of Zr, thus a Ni:Zr molar ratio of 1.5:6. The decrease in BET surface areas for **Ni-1@NU-1000** (1354 $m^2\ g^{-1}$) and **Ni-2@NU-1000** (1282 $m^2\ g^{-1}$) in comparison to as-synthesized NU-1000 (1970 $m^2\ g^{-1}$)[31] is in agreement with the grafting of the Ni complexes into the pores of the material.

SEM images and X-ray absorption near edge structure (XANES) spectra of **Ni-1@NU-1000** were measured. On the basis of this evidence and literature precents,[29-32] we propose that one [NiHSi(*o*-$C_6H_4CH_2PPh_2)_3$] fragment is bound to a [$Zr_6(\mu_3$-$O)_4(\mu_3$-$OH)_4(OH)_4(H_2O)_4]^{8+}$ cluster through the O atom of a hydroxyl ligand.

Catalytic hydroboration by Ni-1 and Ni-2 in homogeneous phase and by Ni-1@NU-1000 and Ni-2@NU-1000 in heterogeneous phase.

The catalyzed hydroboration of carbonyl compounds with boranes (R_2B-H) is a selective reaction towards the synthesis of borate esters,[33-35] intermediates for the synthesis of alcohols,[33] and in the formation of new C-C bonds for Suzuki-Miyauri couplings involving related boronic compounds.[36]. The majority of the catalytic systems reported employ transition metals but there are also works employing main-group and rare earth catalysts. Several recently published reviews of the field summarize the most important developments.[34, 37, 38] Ni is amongst the first-row transition metals that promote hydroboration of aldehydes[39-41] and the more challenging ketone hydroboration (**Tables 1** and **2**).[39, 41-43] Only a limited number of recyclable heterogeneous catalysts have been reported centered on either Fe[44] or Co[45], while MOFs bearing

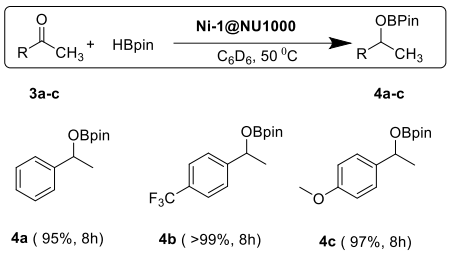

Chart 3. NMR yields of catalysed hydroboration of ketones with pinacolborane.

Ti(IV)[46] and Co(II)[47] sites are also effective for ketone functionalization.

We investigated the catalyzed hydroboration of aldehydes and ketones in homogeneous and heterogeneous media by **Ni-1** and **Ni-2,** vis-à-vis their MOF grafted counterparts **Ni-1@NU-1000** and **Ni-2@NU-1000** (**Charts 2** and **3, Tables 1-3** and **S1-5**). We tested the Ni catalysed pinacolborane hydroboration of ten aliphatic and aromatic aldehydes (**1a-j, Chart 2**) including those with electron-withdrawing and electron-donating substituents, to the corresponding organoborate compounds, **2a-j** (**Chart 2**). We also investigated the hydroboration of three methyl ketones, **3a-c** to the methylborate compounds **4a-c** (**Chart 3**).

The optimization of the catalytic conditions using 4-CF_3-benzaldehyde with **Ni-1** rendered benzene-d_6 as the most suitable solvent over deuterated toluene, chloroform and acetonitrile as solvents (**Tables 3** and **S1**). The reaction was investigated at 25 and 50 °C with different **Ni-1** catalyst loadings: 2, 0.3 and 0.1 mol% (**Tables 3** and **S1**). Although the reactions using **Ni-1** proceeded at room temperature and at lower loadings (0.3 and 0.1 mol%, **Table S1**), we decided to employ 2 mol% of **Ni-1** and 50 °C to obtain reasonable conversions times throughout the substrate scope.

The catalysed reactions proceeded quantitatively with excellent yields across the range of aldehydes used as shown in **Charts 2** and **S2**. The conversions were completed at comparable times when employing MOF supported catalyst **Ni-1@NU-1000**, mostly between 4-5 h for the benzaldehyde series with *p*-substituents spanning from H, Me, ^{t}Bu, OMe to CF_3 (**1a-e**). However, catalysis with **Ni-1@NU-1000** proceeds at room temperature with only 0.3 mol% of Ni as reported in **Chart 2**. We also verified that MOF NU-1000 is inactive under the catalytic conditions (**Table S1**). The hydroborations of aliphatic cyclohexanecarbaldehyde (**1g**), 3-phenylpropanal (**1i**), and heptanal (**1j**) also proceed to completion within 4-4.5 h in the heterogeneous cases while 6 h were needed for the homogenous catalysis. The catalysis of cinnamaldehyde (**1h**) proceeded selectively to the carbonyl hydroboration product with either the homogeneous or heterogeneous catalyst as did that of the 1-methyl-1*H*-pyrrole-2-carbaldehyde (**1f**). No evidence of double bond hydroboration was found. The hydroborations of both **1f** and **1h**, by **Ni-1@NU-1000** are completed in half the time as those by **Ni-1** even carried out at lower temperature and Ni loading. The hydroboration of the pyrrole carbaldehyde (**1f**) is the slowest of the aldehydes tested, taking 6 h to be completed when using the heterogenous system. This is in line with other literature reports informing slower kinetics for the hydroboration of pyridine carbaldehydes.[46 48]

Table 2, entries 1 and 2 show the TON values for the benzaldehyde hydroboration by **Ni-1** (50 °C, TON = 50) and **Ni-1@NU-1000** (25 °C, TON = 333), *ca.* 7 times larger for the heterogeneous system. Furthermore, a direct comparison of the catalytic activity of **Ni-1** and **Ni-1@NU-1000** can be found in **Table 3**, where entries 5 and 6 show a direct comparison of the **Ni-1** catalysts under the same reaction conditions and at the same catalyst loading at room temperature for the catalytic hydroboration of *p*-trifluoromethylbenzaldehyde. The reaction is completed by **Ni-1@NU-1000** after 4 h at room temperature, whereas it has only proceeded to 24% product yield when using homogeneous **Ni-1**.

Our results suggest that the activity of the heterogenous catalyst is not lost after recycling. Thus, for the hydroboration of *p*-trifluoromethylbenzaldehyde, the catalyst **Ni-1@NU-1000** was recovered (by centrifugation and filtration, **Chart S6**, **Table S2**) and its catalytic activity re-evaluated in the same reaction and conditions. To impose harsher conditions this behavior was monitored hourly during three cycles at 50 °C finding that the catalytic activity is not hampered.

In comparison with other reported Ni systems, **Ni-1@NU-1000** as catalyst exhibits the second highest TON value, only outweighed by [Ni(bpy)(cod)], as shown in **Table 2**.[39] Conversion to products after 0.40 h was reported to proceed to only 85% in the case of [Ni(bpy)(cod)] and the catalyst should

Entry	Catalyst	Solvent	Catalyst loading / mol%	T /°C	NMR yield (%)
1	None	C_6D_6	n/a	25	0
2	**Ni-1**	C_7D_8	2.0	50	78
3	**Ni-1**	$CDCl_3$	2.0	50	42
4	**Ni-1**	C_6D_6	2.0	50	>99
5	**Ni-1**	C_6D_6	0.3	25	24
6	**Ni-1@NU-100**	C_6D_6	0.3	25	>99[b]

Table 3. The catalysed hydroboration of 4-CF_3-benzaldehyde by pinacolborane. Reaction conditions: freshly distilled 4-CF_3-benzaldehyde (0.2 mmol), HBpin (0.3 mmol), catalyst (different mol%), solvent (0.4 mL). The product yields were determined by ^{1}H NMR in the presence of 1,3,5-methoxybenzene (0.2 mmol) as the internal standard. The yields are given after 4 h. n/a = not applicable.

be handled under an inert atmosphere. Catalysis with **Ni-1@NU-1000** proceeds under an aerobic atmosphere and the catalyst can be recycled without loss on its activity.

Aldehyde hydroboration employing the phosphinogermyl **Ni-2** and **Ni-2@NU-1000** catalysts also proceeds with excellent yields and selectivity though requiring longer reaction times than the silicon complexes (**Charts 2, S3** and **S5**). The same trend observed for the silicon derivatives is maintained with the germanium complexes in that heterogenization on NU-1000 increases the catalytic efficiency. For example, the hydroboration of benzaldehyde with **Ni-2** (2 mol%) proceeds selectively and quantitatively and is completed after 20 h whereas employing **Ni-2@NU-1000** (0.5 mol%) allows the catalysis to be completed in only 4.5 h. Thus, again for the

germanium analogue the catalysis proceeds faster and with higher conversions when employing the MOF supported catalyst despite employing a lower metal loading.

The hydroboration of three ketones **3a-c** was also investigated using **Ni-1**. It proceeded to only partial conversion of the substrates even after 24 h of reaction. However, the **Ni-1@NU-1000** catalysed reaction gives good spectroscopic yields after 8 h as shown in **Charts 3** and **S7**. Once again, employment of **Ni-2@NU-1000** led to quantitative and selective product conversion but in longer times. In all cases, the heterogeneous reactions were also performed under aerobic conditions finding no significant differences with those performed under argon. In all cases, control experiments in the absence of the Ni catalysts showed no or very slow addition of HBpin to the substrates in the same conditions.

In comparison with other reported Ni ketone hydroboration catalysts (**Table 2**), our systems show a more modest catalytic activity than [Ni(bpy)(cod)],[39] but overall better than the other reported Ni systems, with the added advantage of the tolerance to an aerobic atmosphere and recyclability.

Moreover, these results show that heterogenization into NU-1000 results in enhanced catalytic activity.

We introduced Ge into the ligand skeleton to make a single variation in the electronic properties of the ligand, specifically the σ-donating/accepting ability of the central group 14 atom in the ligand[49-54], and probe its effect in the catalytic cycle.

Preliminary mechanistic evidence

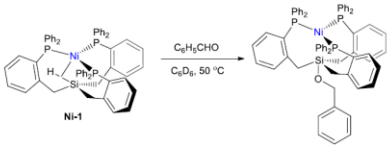

(**Eq. 1**)

Preliminary experimental evidence suggests a transcendental role of the Si-H moiety of the ligand in the hydroboration catalysis by **Ni-1**. The stoichiometric reaction of **Ni-1** with benzaldehyde, proceeded to the formation of a (benzyloxy)tris(benzylphosphine)silane derivative devoid of a Ni-Si bond which was fully characterized (**Equation 1** and ESI section 14). These results are in line with previous observations of the catalytic hydroboration activity of Si(IV) hydride [PhC(N^{t}Bu)$_2$SiHCl$_2$] involving the interaction of the O atom of the aldehyde with the Si atom.[55] Moreover, the addition of allenes to the Pd(η^2-SiH) pincer complex [(PPh$_3$)Pd{Ph$_2$P(*o*-C$_6$H$_4$)}$_2$SiMeH] results in the formation of a complex with a functionalized allylsilane moiety where the Si atom is no longer bonded to Pd, proposed to result from the reductive elimination of the functionalized silane.[56] These indications point to the critical role of Si (or Ge) atom of the Ni complex in the catalytic cycle. We are currently performing more in-depth mechanistic investigations including DFT computations for the hydroboration by **Ni-1** and **Ni-2**. The findings will be reported in due course.

Experimental part

General synthetic procedures.

The syntheses of ligands, metal precursors, and MOF materials were performed under an argon atmosphere using standard Schlenk methods or in an MBraun glove box. Laboratory solvents including hexane, THF, and toluene were dried and purified over MBraun column systems. The synthesis of L1 was previously reported by Stobart and co-workers although not all the spectroscopic features were given in the original publication[14] and we include them in the ESI. $CDCl_3$ was passed through a Pasteur pipette containing molecular sieves and basic alumina and then degassed via three cycles of freeze-pump-thaw, and stored over molecular sieves. Benzene-d_6 and other deuterated solvents were stored over molecular sieves and degassed via three freeze–pump–thaw cycles. Commercial reagents were purchased from Fisher Scientific, Sigma Aldrich, and Oakwood Chemicals and used as received. Nuclear magnetic resonance (NMR) experiments were performed on either Bruker Avance III 300 MHz, 500 MHz, or 600 MHz spectrometers operating with frequency, deuterated solvent, and temperature indicated. Chemical shifts (δ) are reported in parts per million (ppm). ^{1}H NMR spectra for integration were acquired with long delays (30 s). Infra-red spectra were recorded on a Bruker Alpha II ATR-FTIR instrument under nitrogen and are reported in cm^{-1}. Elemental Analysis (C, H) were carried out in an Elementar Unicube analyzer. For ICP-MS determinations, a Perkin Elmer ELAN DRC II ICP-MS instrument was used. X-ray single crystal diffractions were performed on a Bruker D8 Venture instrument with Co/Mo source. Powder X-ray diffraction measurements were done using an AXRD Benchtop from PROTO Manufacturing. X-ray absorption fine structure (XAFS) spectra were measured at the Ni K edge on the **Ni-1@NU-1000** and **Ni-2@NU-1000** materials at the Materials Research Collaborative Access Team (MR-CAT) beamline 10-ID at Argonne National Laboratory's Advanced Photon Source. Samples were prepared in an air-free glovebox as self-supported pressed pellets and were measured in transmission mode in a triple-sealed sample holder to minimize leakage of air. High purity Zr was used to prepare the NU-1000. Scanning electron micrographs (SEM) images were taken using a JEOL 6500F Field Emission SEM at the Institute for Imaging and Analytical Technologies (I^{2}AT Mississippi State University). EDS line scans were also obtained on the same instrument.

Synthesis of tripodal ligand HGe(*o*-C$_6$H$_4$CH$_2$P(C$_6$H$_5$)$_2$)$_3$, L2.

In a Schlenk flask, 1.0 g (3.6 mmol) of diphenyl(*o*-tolyl)phosphine was dissolved in 100 mL of hexane with vigorous stirring for 10 minutes. Then, at –80 °C, 0.6 mL (3.9 mmol) of TMEDA, followed by 1.6 mL (3.9 mmol) of *n*BuLi were added to the phosphine solution, and the mixture was left to reach room temperature and continued to be stirred for a total of 18 hours. The resulting suspension was dried under the vacuum to afford an orange-red colour solid that was redissolved in THF (30 mL). Afterward, 0.31 g of germanium (II) chloride dioxane (1.3 mmol) in THF (30 mL) was added to the slurry solution at -80 °C. The red coloured mixture was stirred for 18 hours at room temperature. Excess water (0.2 mL) was added to the solution producing a clear solution and the mixture was stirred for 1 hour at room temperature. The mixture was then purified by a silica/celite flash chromatography column

using toluene (30 mL) as eluent. After the removal of the volatiles using reduced pressure, the compound was obtained as a crystalline solid (0.72 g, 60 % yield). **^{1}H NMR (500 MHz, C_6D_6, 298 K):** δ 7.37-7.26 (m, 12H, CH_{arom}), 7.03-6.92 (m, 27H, CH_{arom}), 6.83 (t, J_{HH} = 7.3 Hz, 3H, CH_{arom}), 4.75 (m, 1H, H-Ge), 2.92 (d, J_{HH} = 2.4 Hz, 6H, CH_2) ppm. **^{13}C{^{1}H} NMR (150.92 MHz, C_6D_6, 298 K):** 146.6 (d, J_{CP} 27.4 Hz, *C_{ipso}*), 137.6 (d, J_{CP} = 11.5 Hz, *C_{ipso}*), 134.8 (d, J_{CP} = 11.4 Hz, *C_{ipso}*), 134.4 (d, J_{CP} = 19.9 Hz, CH_{arom}), 134.2 (s, CH_{arom}), 129.8 (d, J_{CP} = 4.9 Hz, CH_{arom}), 129.4 (s, CH_{arom}), 128.8 (d, J_{CP} = 7.0 Hz, CH_{arom}), 128.7 (s, CH_{arom}), 128.6 (s, CH_{arom}), 128.4 (s, CH_{arom}), 125.3 (s, CH_{arom}), 22.9 (dt, J_{CP} = 22.7, 2.9 Hz, CH_2) ppm. **^{31}P{^{1}H} NMR (202.5 MHz, C_6D_6, 298 K):** −14.2 (s) ppm. **IR**: 2065 cm^{-1} (*s*, νGe-H). **Anal. Calc.** for $C_{57}H_{49}P_3Ge$: C: 76.10%, H: 5.49%; Found: C: 75.99%, H: 6.05%.

Synthesis of [{$(C_6H_5)_2PCH_2C_6H_4)_3Si$}NiH] (Ni-1).

In a Schlenk flask, 100 mg (0.12 mmol) of **L1** was dissolved in 4.5 mL of dry THF under stirring. A solution of 130 mg (0.12 mmol) of $Ni(PPh_3)_4$ in 4.5 mL of dry THF was added dropwisely and the resulting solution was further stirred at room temperature for 12 h. The reaction mixture changes its color to red, and a yellow precipitate starts to form. After removal of the volatiles under reduced pressure, the residue was washed three times with portions of 4 mL of cold THF and dried under vacuum for 6 hours. Pure compound **Ni-1** was isolated as a yellow solid in 53% yield (57 mg, 0.061 mmol). Yellow crystals suitable for X-ray analysis were obtained by slow evaporation of a benzene-d_6 solution at room temperature. **^{1}H NMR (500 MHz, C_6D_6, 298 K):** δ 7.93 – 7.65 (m, 10H, CH_{arom}), 6.99 (d, $^{2}J_{HH}$= 7.7 Hz, 4H, CH_{arom}), 6.93 (td, $^{2}J_{HH}$= 7.4, $^{3}J_{HP}$= 1.4 Hz, 4H, CH_{arom}), 6.91 – 6.82 (m, 18H, CH_{arom}), 6.81 – 6.72 (m, 3H, CH_{arom}), 6.65 (t, $^{2}J_{HH}$= 7.4 Hz, 3H, CH_{arom}), 2.08 (s, 6H, CH_2), −6.69 (q, $^{2}J_{HP}$ = 37.2 Hz, $J_{H\text{-}Si}$ = 52.0 Hz, 1H, Ni-H) ppm. **^{13}C{^{1}H} NMR (150.9 MHz, C_6D_6, 298 K):** 191.3 (s, *C_{ipso}*), 146.3 (dd, J_{CP} = 9.3, 4.8 Hz, *C_{ipso}*), 138.26 (m, *C_{ipso}*), 134.7 (s, CH_{arom}), 132.5 (d, J_{CP} = 8.8 Hz, *C_{ipso}*), 132.0 (s, CH_{arom}), 131.6 (s, CH_{arom}), 130.4 (s, CH_{arom}), 129.2 (s, CH_{arom}), 128.8 (s, CH_{arom}), 128.7 (d, J_{CP} = 6.8Hz, CH_{arom}), 124.3 (s, CH_{arom}), 27.9 (m, CH_2) ppm. **^{31}P{^{1}H} NMR (202.46 MHz, C_6D_6, 298 K):** 36.9 (s, J_{PSi} = 29.4 Hz) ppm. **DEPT ^{29}Si{^{1}H} NMR (99.36 MHz, C_6D_6, 298 K):** 66.1 (q, J_{SiP} =29.4 Hz) ppm. **IR**: 1885 cm^{-1} (*s*, Ni-H). **Anal. Calc.** for $C_{57}H_{49}NiP_3Si$: C: 74.93%, H: 5.41%; found: C: 74.77%, H: 5.91%.

Synthesis of [{$(C_6H_5)_2PCH_2C_6H_4)_3Ge$}NiH] (Ni-2).

In a Schlenk flask, 24 mg (0.027 mmol) of **L2** was dissolved in 1 mL of dry THF with stirring. A solution of 30 mg (0.027 mmol) of $Ni(PPh_3)_4$ in 1 mL of dry THF was added drop wisely and the resulting solution was stirred at room temperature for 12 h. The reaction mixture changes its colour to red and small amounts of a yellow precipitate form. After removal of the volatiles under reduced pressure, the residue was washed three times with portions of 1 mL of cold THF and dried in vacuum for 6 hours. Compound **Ni-2** was isolated as a yellow solid (23 mg, 89% yield). Yellow crystals suitable for X-ray analysis were obtained by slow evaporation of a benzene-d_6 solution at room temperature. **^{1}H NMR (500 MHz, C_6D_6, 298 K):** δ 8.03 – 7.67 (m, 10H, CH_{arom}), 7.05 – 7.00 (m, 4H, CH_{arom}), 6.93 (td, $^{2}J_{HH}$= 7.4, $^{3}J_{HP}$= 1.3 Hz, 4H, CH_{arom}), 7.00 – 6.81 (m, 18H, CH_{arom}), 6.80 – 6.76 (m, 3H, CH_{arom}), 6.63 (t, $^{2}J_{HH}$= 7.2 Hz, 3H, CH_{arom}), 2.16 (s, 6H, CH_2), -8.15 (q, $^{2}J_{HP}$ = 35.0 Hz, 1H, Ni-H) ppm. **^{13}C{^{1}H} NMR (150.9 MHz, C_6D_6, 298 K):** 147.4 (dd, J_{CP} = 10.8, 5.3 Hz, *C_{ipso}*), 135.4 (q, J_{CP} = 5.1 Hz, CH_{arom}), 134.2 (d, J_{CP} = 19.7 Hz, *C_{ipso}*), 133.8 (s, CH_{arom}), 133.3 (dd, J_{CP} = 20.4, 8.5 Hz, *C_{ipso}*), 130.3 (s, CH_{arom}), 130.0 (s, CH_{arom}), 129.7 (s, CH_{arom}), 124.9 (s, CH_{arom}), 25.5 (m, CH_2) ppm. **^{31}P{^{1}H} NMR (202.46 MHz, C_6D_6, 298 K):** 36.4 (s) ppm. **Anal. Calc.** for $C_{57}H_{49}NiP_3Ge.C_6H_6$: C: 73.01%, H: 5.35%; found: C: 73.09%, H: 5.31%.

Synthesis of grafted material Ni-1@NU-1000.

Microcrystalline NU-1000 (56.1 mg, 0.03 mmol) was added to a 5 mL toluene solution of **Ni-1** (60.6 mg, 0.07 mmol) at room temperature. After stirring for 48 h, the resultant yellow solid was centrifuged out of the suspension and washed with toluene and pentane 4-5 times. The solid was soaked overnight in 3 mL toluene and finally dried under dynamic vacuum for 12 h. The Ni and Zr metal contents in the Ni-1@NU-1000 material were measured in an inductively coupled plasma-mass spectrometer (ICP-MS), finding a 0.560 wt% of Ni and 5.41 wt% of Zr, corresponding to a molar ratio of 0.960 : 6.00 respectively.

Synthesis of grafted material Ni-2@NU-1000.

Microcrystalline NU-1000 (77.7 mg, 0.037 mmol) was added to a 5 mL toluene solution of **Ni-2** (87.8 mg, 0.092 mmol) at room temperature. After stirring for 48 h, the resultant yellow solid was centrifuged out of the suspension and washed with toluene and pentane 4-5 times. The solids were soaked overnight in 3 mL toluene and finally dried under dynamic vacuum for 12 h. The Ni and Zr metal contents in the Ni-2@NU-1000 material by ICP-MS, revealed a 1.02 wt% of Ni and 6.11 wt.% of Zr, corresponding to a molar ratio of 1.56 : 6.00 respectively.

Stoichiometric reaction of Ni-1 and benzaldehyde.

An NMR tube equipped with a J. Young valve was charged with **Ni-1** (0.037 g, 0.049 mmol) and 0.4 mL of C_6D_6. Then 10 μL (0.098 mmol) of benzaldehyde was added. The reaction mixture was heated to 50 °C. The colour of the solution changed to red, and it was analysed by NMR spectroscopy. The Ni complex shown below was isolated as a red solid (0.015 g, 36% yield). ^{1}H NMR (500 MHz, C_6D_6, 298 K): δ 8.38 (s, 5H, CH_{arom}), 7.55 – 7.37 (m, 6H, CH_{arom}), 7.27 (t, $^{2}J_{H\text{-}H}$= 7.6 Hz, 3H, CH_{arom}), 7.15 – 6.98 (m, 19H, CH_{arom}), 6.89 (td, $^{2}J_{H\text{-}H}$= 7.4, 1.4 Hz, 6H, CH_{arom}), 6.67 (t, $^{2}J_{H\text{-}H}$= 7.5 Hz, 3H, CH_{arom}), 4.82 (m, 2H, -OCH_2), 2.78 (s, 3H, CH_2), 2.02 (s, 3H, CH_2) ppm. **^{13}C{^{1}H} NMR (150.9 MHz, C_6D_6, 298 K):** 142.6 (dd, $J_{C\text{-}P}$= 9.5, 5.6 Hz, C_{ipso}), 141.6 (s, CH_{arom}), 137.9 (s, CH_{arom}), 134.6 (dd, $J_{C\text{-}P}$= 20.2, 16.7 Hz, C_{ipso}), 132.3 (s, CH_{arom}), 130.8 (s, CH_{arom}), 128.7 (s, CH_{arom}), 127.4 (s, CH_{arom}), 126.6 (s, CH_{arom}), 124.4 (s, CH_{arom}), 65.2 (s, -OCH_2), 22.5 (m, CH_2) ppm. **^{31}P{^{1}H} NMR (202.46 MHz, C_6D_6, 298 K):** 20.76 (s) ppm. DEPT **^{29}Si{^{1}H} NMR (99.36 MHz, C_6D_6, 298 K):** 10.56 (s) ppm. **Anal. Calc.:** for $C_{64}H_{55}NiP_3SiO$: C: 75.37%, H: 5.44%; Found: C: 74.98%, H: 5.51%.

Catalytic studies

The catalytic optimization conditions and findings are described in detail in the supporting information (section 13).

DFT computations

To support the structural characterization, DFT (density functional theory) computations were performed to simulate the hydride signal in the ^{1}H NMR spectra, allowing to distinguish between a classical hydride and a non-classical σ-silane or germane using the Gaussian 16 software.[57] The geometries,

first, were optimized using the PBE1PBE functional with the damping dispersion correction[11] at the BS1 level of theory. In BS1, 6-31(d')[58-60] basis set is used for C and H atoms and modified LanL2DZ+ECP[61-63] is used for Ni, Si, P, and Ge atoms. Single-point calculations associated with Gauge-Independent Atomic Orbital (GIAO)[64] with the same functional at BS2 basis set were carried out on the gas phase geometries to obtain chemical shifts. At the basis set BS2, 6-311+G(d,p)[65, 66] is used for C and H atoms and modified LanL2DZ is used for Ni, Si, P, and Ge atoms. In the single point calculations, solvent effect of benzene were also included with Solvation Model Based on Density (SMD)[67] calculations. The final results reported at SMD(benzene)-PBE1PBE-D3/BS2//PBE1PBE-D3/BS1 level theory are shown in **Figures S1** and **S2.**

Conclusions

In conclusion, preliminary catalytic results on the hydroboration of aldehydes and ketones by **Ni-1@NU-1000** show a seven-fold increase in the TON by grafting the organometallic precursor **Ni-1** into the MOF material. The same trend was observed in **Ni-2@NU-1000** by comparison with **Ni-2**. The supported materials can be handled under air and be recycled a few times with no apparent decrease in the catalytic properties. The presence of Ge in the ligand decreases the catalytic activity but does not affect the selectivity of the reaction. In sum, not only the catalytic activity but also the robustness of the catalyst are benefited by grafting of the organometallic into the MOF material.

Conflicts of interest

There are no conflicts to declare.

Acknowledgements

We are grateful for the generous financial support of the National Science Foundation (CHE 2102689 and CHE 2102552). Work at Argonne National Laboratory was supported by the U.S. Department of Energy (DOE), Office of Basic Energy Sciences, Division of Chemical Sciences, Geosciences, and Biosciences, Catalysis Science Program under contract No. DE-AC-02-06CH11357. Use of the Advanced Photon Source is supported by the U.S. Department of Energy, Office of Science, and Office of the Basic Energy Sciences, under Contract No. DE-AC-02−06CH11357. We thank Dr. Saidulu Gorla for initial work, Dr. Joshua Wright and Dr. A. Jeremy Kropf (ANL) for assistance in collecting and interpreting XAFS spectra, and Dr. Rooban Venkatesh K. G. Thirumalai at I²AT Mississippi State for collecting SEM-EDS data.

Notes and references

1. O. M. Yaghi, G. Li and H. Li, "Selective binding and removal of guests in a microporous metal–organic framework," *Nature*, 1995, **378**, 703-706.

2. Z. Chen, X. Yan, M. Li, S. Wang and C. Chen, "Defect-Engineered Chiral Metal–Organic Frameworks for Efficient Asymmetric Aldol Reaction," *Inorganic Chemistry*, 2021, **60**, 4362-4365.

3. D. Chen, R. Luo, M. Li, M. Wen, Y. Li, C. Chen and N. Zhang, "Salen(Co(iii)) imprisoned within pores of a metal–organic framework by post-synthetic modification and its asymmetric catalysis for CO2 fixation at room temperature," *Chemical Communications*, 2017, **53**, 10930-10933.

4. R. A. Peralta, M. T. Huxley, P. Lyu, M. L. Díaz-Ramírez, S. H. Park, J. L. Obeso, C. Leyva, C. Y. Heo, S. Jang, J. H. Kwak, G. Maurin, I. A. Ibarra and N. C. Jeong, "Engineering Catalysis within a Saturated In(III)-Based MOF Possessing Dynamic Ligand–Metal Bonding," *ACS Applied Materials & Interfaces*, 2023, **15**, 1410-1417.

5. A. E. Platero-Prats, A. Mavrandonakis, J. Liu, Z. Chen, Z. Chen, Z. Li, A. A. Yakovenko, L. C. Gallington, J. T. Hupp, O. K. Farha, C. J. Cramer and K. W. Chapman, "The Molecular Path Approaching the Active Site in Catalytic Metal–Organic Frameworks," *Journal of the American Chemical Society*, 2021, **143**, 20090-20094.

6. G. Bauer, D. Ongari, D. Tiana, P. Gaumann, T. Rohrbach, G. Pareras, M. Tarik, B. Smit and M. Ranocchiari, "Metal-organic frameworks as kinetic modulators for branched selectivity in hydroformylation," *Nat. Commun.*, 2020, **11**, 1059.

7. L. Jiao, J. Wang and H.-L. Jiang, "Microenvironment Modulation in Metal–Organic Framework-Based Catalysis," *Accounts of Materials Research*, 2021, **2**, 327-339.

8. Z. H. Syed, F. Sha, X. Zhang, D. M. Kaphan, M. Delferro and O. K. Farha, "Metal–Organic Framework Nodes as a Supporting Platform for Tailoring the Activity of Metal Catalysts," *ACS Catalysis*, 2020, **10**, 11556-11566.

9. D. Yang and B. C. Gates, "Catalysis by Metal Organic Frameworks: Perspective and Suggestions for Future Research," *ACS Catalysis*, 2019, **9**, 1779-1798.

10. T. C. Wang, N. A. Vermeulen, I. S. Kim, A. B. F. Martinson, J. F. Stoddart, J. T. Hupp and O. K. Farha, "Scalable synthesis and post-modification of a mesoporous metal-organic framework called NU-1000," *Nature Protocols*, 2016, **11**, 149.

11. Z. Li, N. M. Schweitzer, A. B. League, V. Bernales, A. W. Peters, A. B. Getsoian, T. C. Wang, J. T. Miller, A. Vjunov, J. L. Fulton, J. A. Lercher, C. J. Cramer, L. Gagliardi, J. T. Hupp and O. K. Farha, "Sintering-Resistant Single-Site Nickel Catalyst Supported by Metal–

Organic Framework," *Journal of the American Chemical Society*, 2016, **138**, 1977-1982.

12. Y.-S. Wei, M. Zhang, R. Zou and Q. Xu, "Metal–Organic Framework-Based Catalysts with Single Metal Sites," *Chemical Reviews*, 2020, **120**, 12089-12174.

13. M. Dincă, F. P. Gabbaï and J. R. Long, "Organometallic Chemistry within Metal–Organic Frameworks," *Organometallics*, 2019, **38**, 3389-3391.

14. R. A. Gossage, G. D. McLennan and S. R. Stobart, "(Phosphinoalkyl)silanes. 3.1 Poly(o-(diphenylphosphino)benzyl)silanes: Synthesis, Spectroscopic Properties, and Complexation at Platinum or Iridium," *Inorganic Chemistry*, 1996, **35**, 1729-1732.

15. E. Rufino-Felipe, M.-Á. Muñoz-Hernández and V. Montiel-Palma, "Lithium Complexes Derived of Benzylphosphines: Synthesis, Characterization and Evaluation in the ROP of rac-Lactide and ε-Caprolactone," *Molecules*, 2018, **23**, 82.

16. R. J. Cross and F. Glockling, "Infrared spectra of organogermanes," *Journal of Organometallic Chemistry*, 1965, **3**, 146-155.

17. R. Herrmann, T. Braun and S. Mebs, "[Ge(H)(2-C6H4PPh2)3] as Ligand Precursor at Ruthenium: Formation and Reactivity of [Ru(Cl){Ge(2-C6H4PPh2)3}]," *European Journal of Inorganic Chemistry*, 2014, **2014**, 4826-4835.

18. M. T. Whited, N. P. Mankad, Y. Lee, P. F. Oblad and J. C. Peters, "Dinitrogen Complexes Supported by Tris(phosphino)silyl Ligands," *Inorg. Chem.*, 2009, **48**, 2507-2517.

19. C. Tsay and J. C. Peters, "Thermally stable N2 and H2 adducts of cationic nickel(II)," *Chem. Sci.*, 2012, **3**, 1313-1318.

20. J. Takaya and N. Iwasawa, "Reaction of bis(o-phosphinophenyl)silane with M(PPh3)4 (M = Ni, Pd, Pt): synthesis and structural analysis of [small eta]2-(Si-H) metal(0) and pentacoordinate silyl metal(ii) hydride complexes of the Ni triad bearing a PSiP-pincer ligand," *Dalton Transactions*, 2011, **40**, 8814-8821.

21. H.-W. Suh, L. M. Guard and N. Hazari, "Synthesis and reactivity of a masked PSiP pincer supported nickel hydride," *Polyhedron*, 2014, **84**, 37-43.

22. B. A. Connor, J. Rittle, D. VanderVelde and J. C. Peters, "A Ni(0)(η2-(Si-H))(η2-H2) Complex That Mediates Facile H Atom Exchange between Two σ-Ligands," *Organometallics*, 2016, **35**, 686-690.

23. M. Tanabe, R. Yumoto and K. Osakada, "Reaction of an alkyne with dinickel-diphenylsilyl complexes. An emissive disilane formed via the consecutive Si-C and Si-Si bond-making processes," *Chemical Communications*, 2012, **48**, 2125-2127.

24. J. Y. Corey and J. Braddock-Wilking, "Reactions of Hydrosilanes with Transition-Metal Complexes: Formation of

Stable Transition-Metal Silyl Compounds," *Chemical Reviews*, 1999, **99**, 175-292.

25. J. A. Cabeza, P. García-Álvarez, C. J. Laglera-Gándara and E. Pérez-Carreño, "Dipyrromethane-Based PGeP Pincer Methylgermyl and Methoxidogermyl Nickel and Palladium Complexes," *European Journal of Inorganic Chemistry*, 2021, **2021**, 1897-1902.

26. H.-W. Suh, D. Balcells, A. J. Edwards, L. M. Guard, N. Hazari, E. A. Mader, B. Q. Mercado and M. Repisky, "Understanding the Solution and Solid-State Structures of Pd and Pt PSiP Pincer-Supported Hydrides," *Inorganic Chemistry*, 2015, **54**, 11411-11422.

27. D. J. Charboneau, D. Balcells, N. Hazari, H. M. C. Lant, J. M. Mayer, P. R. Melvin, B. Q. Mercado, W. D. Morris, M. Repisky and H.-W. Suh, "Dinitrogen-Facilitated Reversible Formation of a Si–H Bond in a Pincer-Supported Ni Complex," *Organometallics*, 2016, **35**, 3154-3162.

28. T. Islamoglu, K.-i. Otake, P. Li, C. T. Buru, A. W. Peters, I. Akpinar, S. J. Garibay and O. K. Farha, "Revisiting the structural homogeneity of NU-1000, a Zr-based metal–organic framework," *CrystEngComm*, 2018, **20**, 5913-5918.

29. S. P. Desai, J. Ye, J. Zheng, M. S. Ferrandon, T. E. Webber, A. E. Platero-Prats, J. Duan, P. Garcia-Holley, D. M. Camaioni, K. W. Chapman, M. Delferro, O. K. Farha, J. L. Fulton, L. Gagliardi, J. A. Lercher, R. L. Penn, A. Stein and C. C. Lu, "Well-Defined Rhodium–Gallium Catalytic Sites in a Metal–Organic Framework: Promoter-Controlled Selectivity in Alkyne Semihydrogenation to E-Alkenes," *Journal of the American Chemical Society*, 2018, **140**, 15309-15318.

30. A. B. Thompson, D. R. Pahls, V. Bernales, L. C. Gallington, C. D. Malonzo, T. Webber, S. J. Tereniak, T. C. Wang, S. P. Desai, Z. Li, I. S. Kim, L. Gagliardi, R. L. Penn, K. W. Chapman, A. Stein, O. K. Farha, J. T. Hupp, A. B. F. Martinson and C. C. Lu, "Installing Heterobimetallic Cobalt–Aluminum Single Sites on a Metal Organic Framework Support," *Chemistry of Materials*, 2016, **28**, 6753-6762.

31. S. Gorla, M. L. Díaz-Ramírez, N. S. Abeynayake, D. M. Kaphan, D. R. Williams, V. Martis, H. A. Lara-García, B. Donnadieu, N. Lopez, I. A. Ibarra and V. Montiel-Palma, "Functionalized NU-1000 with an

Iridium Organometallic Fragment: SO2 Capture Enhancement," *ACS Applied Materials & Interfaces*, 2020, **12**, 41758-41764.

32. J. Garcia Ponce, M. L. Diaz-Ramirez, S. Gorla, C. Navarathna, G. Sanchez-Lecuona, B. Donnadieu, I. A. Ibarra and V. Montiel-Palma, "SO2 capture enhancement in NU-1000 by the incorporation of a ruthenium gallate organometallic complex," *CrystEngComm*, 2021, **23**, 7479-7484.

33. M. L. Shegavi and S. K. Bose, "Recent advances in the catalytic hydroboration of carbonyl compounds," *Catalysis Science & Technology*, 2019, **9**, 3307-3336.

34. S. J. Geier, C. M. Vogels, J. A. Melanson and S. A. Westcott, "The transition metal-catalysed hydroboration reaction," *Chemical Society Reviews*, 2022, **51**, 8877-8922.

35. L. Xu, G. Wang, S. Zhang, H. Wang, L. Wang, L. Liu, J. Jiao and P. Li, "Recent advances in catalytic C–H borylation reactions," *Tetrahedron*, 2017, **73**, 7123-7157.

36. T. Gensch, S. R. Smith, T. J. Colacot, Y. N. Timsina, G. Xu, B. W. Glasspoole and M. S. Sigman, "Design and Application of a Screening Set for Monophosphine Ligands in Cross-Coupling," *ACS Catal.*, 2022, **12**, 7773-7780.

37. M. L. Shegavi and S. K. Bose, "Recent advances in the catalytic hydroboration of carbonyl compounds," *Catal. Sci. Technol.*, 2019, **9**, 3307-3336.

38. M. Magre, M. Szewczyk and M. Rueping, "s-Block Metal Catalysts for the Hydroboration of Unsaturated Bonds," *Chemical Reviews*, 2022, **122**, 8261-8312.

39. A. E. King, S. C. E. Stieber, N. J. Henson, S. A. Kozimor, B. L. Scott, N. C. Smythe, A. D. Sutton and J. C. Gordon, "Ni(bpy)(cod): A Convenient Entryway into the Efficient Hydroboration of Ketones, Aldehydes, and Imines," *European Journal of Inorganic Chemistry*, 2016, **2016**, 1635-1640.

40. I. Hossain and J. A. R. Schmidt, "Nickel(II) Catalyzed Hydroboration: A Route to Selective Reduction of Aldehydes and N-Allylimines," *European Journal of Inorganic Chemistry*, 2020, **2020**, 1877-1884.

41. K. A. Gudun, M. Segizbayev, A. Adamov, P. N. Plessow, K. A. Lyssenko, M. P. Balanay and A. Y. Khalimon, "POCN Ni(ii) pincer complexes: synthesis, characterization and evaluation of catalytic hydrosilylation and hydroboration activities," *Dalton Transactions*, 2019, **48**, 1732-1746.

42. A. Flores-Gaspar, P. Pinedo-González, M. G. Crestani, M. Muñoz-Hernández, D. Morales-Morales, B. A. Warsop, W. D. Jones and J. J. García, "Selective hydrogenation of the CO bond of ketones using Ni(0) complexes with a chelating bisphosphine," *Journal of Molecular Catalysis A: Chemical*, 2009, **309**, 1-11.

43. G. Vijaykumar, M. Bhunia and S. K. Mandal, "A phenalenyl-based nickel catalyst for the hydroboration of olefins under ambient conditions," *Dalton Transactions*, 2019, **48**, 5779-5784.

44. G. Zhang, J. Cheng, K. Davis, M. G. Bonifacio and C. Zajaczkowski, "Practical and selective hydroboration of aldehydes and ketones in air catalysed by an iron(ii) coordination polymer," *Green Chemistry*, 2019, **21**, 1114-1121.

45. J. Wu, H. Zeng, J. Cheng, S. Zheng, J. A. Golen, D. R. Manke and G. Zhang, "Cobalt(II) Coordination Polymer as a Precatalyst for Selective Hydroboration of Aldehydes, Ketones, and Imines," *The Journal of Organic Chemistry*, 2018, **83**, 9442-9448.

46. Z. Huang, D. Liu, J. Camacho-Bunquin, G. Zhang, D. Yang, J. M. López-Encarnación, Y. Xu, M. S. Ferrandon, J. Niklas, O. G. Poluektov, J. Jellinek, A. Lei, E. E. Bunel and M. Delferro, "Supported Single-Site Ti(IV) on a Metal–Organic Framework for the Hydroboration of Carbonyl Compounds," *Organometallics*, 2017, **36**, 3921-3930.

47. K. Manna, P. Ji, Z. Lin, F. X. Greene, A. Urban, N. C. Thacker and W. Lin, "Chemoselective single-site Earth-abundant metal catalysts at metal–organic framework nodes," *Nature Communications*, 2016, **7**, 12610.

48. S. Lau, C. B. Provis-Evans, A. P. James and R. L. Webster, "Hydroboration of aldehydes, ketones and CO2 under mild conditions mediated by iron(iii) salen complexes," *Dalton Transactions*, 2021, **50**, 50, 10696-10700.

49. H. Kameo, S. Ishii and H. Nakazawa, "Synthesis and Reactivity of Rhodium Complexes Bearing [E(o-C6H4PPh2)3]-Type Tetradentate Ligands (E = Si, Ge, and Sn)," *Organometallics*, 2012, **31**, 2212-2218.

50. H. Kameo, S. Ishii and H. Nakazawa, "Facile synthesis of rhodium and iridium complexes bearing a [PEP]-type ligand (E = Ge or Sn) via E-C bond cleavage," *Dalton Transactions*, 2012, **41**, 11386-11392.

51. H. Kameo, S. Ishii and H. Nakazawa, "Synthesis of iridium complexes bearing {o-(Ph2P)C6H4}3E type (E = Si, Ge, and Sn) ligand and evaluation of electron donating ability of group 14 elements E," *Dalton Transactions*, 2012, **41**, 8290-8296.

52. M. A. Bennett, S. K. Bhargava, N. Mirzadeh and S. H. Privér, "The use of [2-C6R4PPh2]– (R = H, F) and related carbanions as building blocks in coordination chemistry," *Coordination Chemistry Reviews*, 2018, **370**, 69-128.

53. P. Gualco, T.-P. Lin, M. Sircoglou, M. Mercy, S. Ladeira, G. Bouhadir, L. M. Pérez, A. Amgoune, L. Maron, F. P. Gabbaï and D. Bourissou, "Gold–Silane and Gold–Stannane Complexes: Saturated Molecules as σ-Acceptor Ligands," *Angewandte Chemie International Edition*, 2009, **48**, 9892-9895.

54. P. Gualco, S. Mallet-Ladeira, H. Kameo, H. Nakazawa, M. Mercy, L. Maron, A. Amgoune and D. Bourissou, "Coordination of a Triphosphine–Silane to Gold: Formation of a Trigonal Pyramidal Complex Featuring Au+→Si Interaction," *Organometallics*, 2015, **34**, 1449-1453.

55. M. K. Bisai, S. Pahar, T. Das, K. Vanka and S. S. Sen, "Transition metal free catalytic hydroboration of aldehydes and aldimines by amidinato silane," *Dalton Transactions*, 2017, **46**, 2420-2424.

56. J. Takaya and N. Iwasawa, "Bis(o-phosphinophenyl)silane as a Scaffold for Dynamic Behavior of H−Si and C−Si Bonds with Palladium(0)," *Organometallics*, 2009, **28**, 6636-6638.

57. M. J. Frisch, G. W. Trucks, H. B. Schlegel, G. E. Scuseria, M. A. Robb, J. R. Cheeseman, G. Scalmani, V. Barone, G. A. Petersson, H. Nakatsuji, X. Li, M. Caricato, A. V. Marenich, J. Bloino, B. G. Janesko, R. Gomperts, B. Mennucci, H. P. Hratchian, J. V. Ortiz, A. F. Izmaylov, J. L. Sonnenberg, Williams, F. Ding, F. Lipparini, F. Egidi, J. Goings, B. Peng, A. Petrone, T. Henderson, D. Ranasinghe, V. G. Zakrzewski, J. Gao, N. Rega, G. Zheng, W. Liang, M. Hada, M. Ehara, K. Toyota, R. Fukuda, J. Hasegawa, M. Ishida, T. Nakajima, Y. Honda, O. Kitao, H. Nakai, T. Vreven, K. Throssell, J. A. Montgomery Jr., J. E. Peralta, F. Ogliaro, M. J. Bearpark, J. J. Heyd, E. N. Brothers, K. N. Kudin, V. N. Staroverov, T. A. Keith, R. Kobayashi, J. Normand, K. Raghavachari, A. P. Rendell, J. C. Burant, S. S. Iyengar, J. Tomasi, M. Cossi, J. M. Millam, M. Klene, C. Adamo, R. Cammi, J. W. Ochterski, R. L. Martin, K. Morokuma, O. Farkas, J. B. Foresman and D. J. Fox, *Gaussian, Inc.,* Wallingford CT, 2016.

58. W. J. Hehre, R. Ditchfield and J. A. Pople, "Self—Consistent Molecular Orbital Methods. XII. Further Extensions of Gaussian—Type Basis Sets for Use in Molecular Orbital Studies of Organic Molecules," *The Journal of Chemical Physics*, 1972, **56**, 2257-2261.

59. P. C. Hariharan and J. A. Pople, "The influence of polarization functions on molecular orbital hydrogenation energies," *Theoretica chimica acta*, 1973, **28**, 213-222.

60. G. A. Petersson and M. A. Al-Laham, "A complete basis set model chemistry. II. Open-shell systems and the total energies of the first-row atoms," *The Journal of Chemical Physics*, 1991, **94**, 6081-6090.

61. P. J. Hay and W. R. Wadt, "Ab initio effective core potentials for molecular calculations. Potentials for K to Au including the outermost core orbitals," *The Journal of Chemical Physics*, 1985, **82**, 299-310.

62. P. J. Hay and W. R. Wadt, "Ab initio effective core potentials for molecular calculations. Potentials for the transition metal atoms Sc to Hg," *The Journal of Chemical Physics*, 1985, **82**, 270-283.

63. M. Couty and M. B. Hall, "Basis sets for transition metals: Optimized outer p functions," *Journal of Computational Chemistry*, 1996, **17**, 1359-1370.

64. R. Ditchfield, "Self-consistent perturbation theory of diamagnetism," *Molecular Physics*, 1974, **27**, 789-807.

65. R. Krishnan, J. S. Binkley, R. Seeger and J. A. Pople, "Self-consistent molecular orbital methods. XX. A basis set for correlated wave functions," *The Journal of Chemical Physics*, 1980, **72**, 650-654.

66. A. D. McLean and G. S. Chandler, "Contracted Gaussian basis sets for molecular calculations. I. Second row atoms, Z=11–18," *The Journal of Chemical Physics*, 1980, **72**, 5639-5648.

67. A. V. Marenich, C. J. Cramer and D. G. Truhlar, "Universal Solvation Model Based on Solute Electron Density and on a Continuum Model of the Solvent Defined by the Bulk Dielectric Constant and Atomic Surface Tensions," *The Journal of Physical Chemistry B*, 2009, **113**, 6378-6396.